OPEN ACCESS
IOP Publishing
Journal of Physics: Condensed Matter
J. Phys.: Condens. Matter **36** (2024) 345402 (9pp)
https://doi.org/10.1088/1361-648X/ad4b83

Approach to hyperuniformity of steady states of facilitated exclusion processes

S Goldstein, J L Lebowitz[1] and E R Speer*

Department of Mathematics, Rutgers University, New Brunswick, NJ 08903, United States of America

E-mail: speer@math.rutgers.edu

Received 16 February 2024, revised 18 April 2024
Accepted for publication 14 May 2024
Published 31 May 2024

Abstract

We consider the fluctuations in the number of particles in a box of size L^d in $\mathbb{Z}^d$, $d \geqslant 1$, in the (infinite volume) translation invariant stationary states of the facilitated exclusion process, also called the conserved lattice gas model. When started in a Bernoulli (product) measure at density ρ, these systems approach, as $t \to \infty$, a 'frozen' state for $\rho \leqslant \rho_c$, with $\rho_c = 1/2$ for $d = 1$ and $\rho_c < 1/2$ for $d \geqslant 2$. At $\rho = \rho_c$ the limiting state is, as observed by Hexner and Levine, hyperuniform, that is, the variance of the number of particles in the box grows slower than L^d. We give a general description of how the variances at different scales of L behave as $\rho \nearrow \rho_c$. On the largest scale, $L \gg L_2$, the fluctuations are normal (in fact the same as in the original product measure), while in a region $L_1 \ll L \ll L_2$, with both L_1 and L_2 going to infinity as $\rho \nearrow \rho_c$, the variance grows faster than normal. For $1 \ll L \ll L_1$ the variance is the same as in the hyperuniform system. (All results discussed are rigorous for $d = 1$ and based on simulations for $d \geqslant 2$.)

Keywords: facilitated exclusion process, conserved lattice gas, hyperuniform states

1. Introduction

An important quantity in the study of particle systems in $\mathbb{Z}^d$ (or $\mathbb{R}^d$) is the fluctuation in the number of particles in a domain D; an indicator of the size of such fluctuations is the variance of the number of particles in D. We will restrict our attention to particle systems on $\mathbb{Z}^d$ in which each lattice site can contain at most one particle. Consider then a translation invariant system in which the probabilities of configurations are described by a measure μ and the particle density is ρ, and let N_L be the number of particles in a cubical domain of size L^d. The expected value of N_L is ρL^d for all L, and we shall denote its variance by $V(L)$. In general $V(L)$ is related to the pair correlation function: $V(L)/L^d \to S(0)$ as $L \to \infty$, where $S(k)$ is the Fourier transform of the total pair correlation function [15].

For many systems of this sort, such as equilibrium systems which are described by a Gibbs measure with integrable potentials and are not at a phase transition, $V(L) \simeq CL^d$ as $L \to \infty$, with C the compressibility. For an ideal lattice gas (i.e. one with no interactions between different lattice sites) in equilibrium, the Gibbs measure μ is a Bernoulli product measure and $C = \rho(1-\rho)$. There are also many cases of interest, such as systems at equilibrium critical points or the voter model in $d > 2$ (for which the result follows from (2.4) of [13]), in which $V(L)$ grows faster than L^d and $S(0)$ is infinite.

Our interest here is in the opposite case, in which $V(L)$ grows more slowly than the volume, i.e. $S(0) = 0$. These are the so called *hyperuniform* systems [15] (originally called super homogeneous systems). In fact we shall restrict our considerations to the particular situation in which the measures studied describe the final stationary states of stochastic lattice systems started from a Bernoulli product measure and evolving according to the *facilitated exclusion process* (FEP) (also called the *conserved lattice gas model*). As we shall

[1] Also Department of Physics, Rutgers.
* Author to whom any correspondence should be addressed.

describe in detail below, these systems undergo a transition from frozen to active final states at some critical density ρ_c, at which density the system is hyperuniform.

The approach to this hyperuniform state as $\rho \to \rho_c$ depends on the direction of approach and is very different, for $\rho \nearrow \rho_c$, from what one might expect in general, which is that the constant $C = C(\rho)$ would approach zero (as in the ideal lattice gas when $\rho \to 1$). Rather, when the approach is from lower densities, $C(\rho)$ continues to have its ideal gas value for all ρ, but the values of L at which the approximation $V(L) \approx C(\rho)L^d$ is valid become larger and larger as $\rho \nearrow \rho_c$. For approach from above we do have $C(\rho) \searrow 0$ as $\rho \searrow \rho_c$. In particular for $d = 1$, where $\rho_c = 1/2$, it follows from (54) of [9] that $C(\rho) = \rho(1-\rho)(2\rho-1)$, since the stationary measure for the lattice model studied there, with particles covering 2 sites, is shown in [1] to coincide with the stationary measure for the FEP at densities $\rho > 1/2$ after interchange of particles and holes.

In the remainder of the paper we first (section 2) introduce the facilitated exclusion systems that we study and review earlier work, in particular the work by Hexner and Levine [8] discussing, for the two-dimensional model, the hyperuniformity of the system at the critical density and the approach to this hyperuniformity as $\rho \nearrow \rho_c$. We then, in section 3, propose a more detailed, but still phenomenological, characterization of the L-dependence of the variances $V(L)$ for $d = 1, 2$, supporting the proposal by a procedure we call *power scaling*. We also present a simple argument, rigorous for $d = 1$, for the fact that in all these models, and at all densities $\rho < \rho_c$, the variance grows as $\rho(1-\rho)L^d$ for sufficiently large L (that is, the prefactor C mentioned above is then $\rho(1-\rho)$).

The proposal in section 3 is based on data from simulations, some new, in two dimensions; in section 4 we describe in more detail the FEP process in $d = 1$. In that case we can establish rigorously a version of the general structure described in $d = 2$. We give exact values for the exponents characterizing the behavior of the variance in different ranges of L; these are different from those in $d = 2$, and in $d = 1$ there is also a difference, for L small, between the exponents for L odd and for L even. In section 5 we give a hint of the rigorous derivation of these results; full proofs will be given elsewhere. In the concluding section we mention results for some other related models and discuss open problems.

2. Facilitated systems

We shall be concerned here primarily with certain stationary states, in $\mathbb{Z}^d$, of the symmetric FEP, also known as the Conserved Lattice Gas process. In this system a site of the lattice can be occupied by at most one particle, and a particle can jump to a neighboring empty site only if it has also an occupied neighbor site.

The stationary states of this system have been investigated numerically for $d \geqslant 2$ [8, 11, 14] and theoretically for $d = 1$ [1–3, 6]. These investigations suggest that the system, when started with an initial random configuration at density ρ, approaches, as $t \to \infty$, either a *frozen* state in which all particles are isolated and hence unable to move, or an *active* stationary state in which there is a finite density of *active* particles: those with an occupied neighboring site. The transition (often called a *transition to an absorbing state* or an *absorbing phase transition*) occurs at a density $\rho_c \leqslant 1/2$ (for $\rho > 1/2$ it is geometrically impossible for all the particles to be isolated). For $d = 1$, $\rho_c = 1/2$, but rather surprisingly, when $d \geqslant 2$ the simulations find values of ρ_c to be much smaller than $1/2$. We discuss below the determination of ρ_c as well as its dependence on which of several different ways the dynamics of the model is defined.

Another surprising observation, due to Hexner and Levine [8], is that, in 2d and 3d, the frozen limiting state of the system at ρ_c is hyperuniform: $V(L) \sim L^{\lambda_1}$, with $\lambda_1 \approx 1.57$ in 2d and $\lambda_1 \approx 2.76$ in 3d [8]. (Throughout we will relate two quantities by '$\simeq$' or, respectively, by '$\sim$' to express the fact that asymptotically their ratio is equal to 1 or, respectively, is bounded away from both 0 and ∞.) Hexner and Levine also discuss in detail how $V(L)$ grows with L for ρ close to, but less than, ρ_c. They find a crossover, as L increases, from a scale on which $V(L)$ grows as L^{λ_1} to a scale on which the growth is as L^d (in each case for L large on the relevant scale). In the current paper we are particularly interested in the transition region between the two behaviors, the location of which moves towards larger values of L as $\rho \nearrow \rho_c$.

Dynamics and the determination of ρ_c: Several different implementations of the dynamics have appeared in the literature. The jumps may occur either in continuous time, with each particle attempting to jump at rate 1, or in discrete time, with all active particles attempting to jump simultaneously at integer times; the target site for the jump can be (1) chosen at random from all neighbors, with a jump occurring only if the chosen site is empty, or (2) chosen at random from just the empty neighbors. (In the discrete time case several particles may attempt to jump to the same site; in this case, one is chosen at random to succeed.) For example, discrete time updating with rule (2) is used in [8, 14]; continuous time updating is used with rule (2) in [11] and with rule (1) both in [12] and, for *exclusion processes* (in which no facilitation is required for a jump), in the mathematical literature of interacting particle systems [10].

To investigate ρ_c for $d = 2$ one simulates the dynamics in a square box in $\mathbb{Z}^2$, with periodic boundary conditions, starting with a random distribution at some density $\rho < 1/2$. In this setting it is easy to show, using the theory of finite state Markov processes, that for any initial state the system *must* eventually freeze. This means that a non-frozen steady state with $\rho < 1/2$ cannot exist in finite volume, and hence that if one were to try to define a critical density for a finite system as we have done for the infinite system, one would find a value of $1/2$. To avoid mentioning this uninteresting result further we reserve the term 'critical density' and the notation ρ_c for the infinite-system value.

Nevertheless, there are several methods for determining an approximate value of ρ_c from such simulations; we discuss two of these. The first method is straightforward, depending only on the observation of dramatic growth in the freezing time for

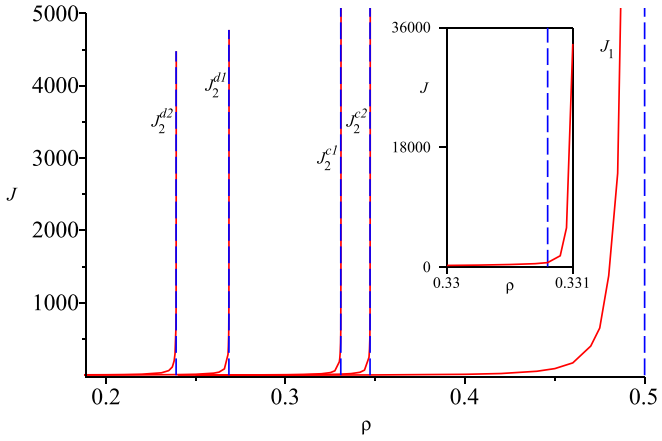

Figure 1. Mean value of the number J of jumps per particle required to freeze the system, versus density ρ, for the 2d FEP with four different dynamics; J_2^{d2} denotes the curve for the distrete time rule (2) model, etc. Also shown, and denoted J_1, are results for the 1d continuous time FEP. The (dashed) vertical lines are at the critical densities. The inset shows an expanded view of the curve J_2^{c1} near its critical value $\rho_c = 0.3308$.

ρ near ρ_c. The second method requires making some assumptions about the behavior of the infinite system as $\rho \searrow \rho_c$. It gives precise values for ρ_c (which depend, however, on the size of the simulated system). For the sake of definiteness we will adopt here the value which we obtain from this method in a box of side $L = 1024$.

The first approach is to count the number of particle jumps required for the system to freeze; for a somewhat vaguely defined density $\tilde{\rho}_c$ this number increases very rapidly as $\rho \nearrow \tilde{\rho}_c$. Let $J = J(\rho)$ be the number of required jumps divided by the number of particles in the system. Figure 1 plots the mean of $J(\rho)$, over 200 trials, against ρ, for the four types of dynamics discussed above; the data are for a box of side $L = 1024$. (We have also shown in this figure the values of ρ_c; clearly one could take $\tilde{\rho}_c = \rho_c$, since the sharp increase in $J(\rho)$ at ρ_c is clear.) For comparison the results of a 1d simulation (in a periodic system of 2^{17} sites) of the continuous time FEP, for which ρ_c is known to have value $1/2$, are also shown.

In fact the situation is not quite as simple as suggested above and by the main part of figure 1: for the 2d models there *is* a sharp increase in J as the critical density is approached, but a much more rapid one just past that density. This is shown, for the continuous time rule (1) model, in the inset. In contrast, for the 1d model the increase occurs well before the critical value.

The second method [11] is first to determine an approximate value of ρ_c, perhaps by the method discussed above, and then to simulate the system at several slightly higher densities. At such densities the simulation will enter a long-lived metastable state which is presumably close to a projection of the infinite-volume active state at that density. Let $\rho_a = \rho_a(\rho)$ denote the density in this state of active particles; then ρ_a vanishes as $\rho \searrow \rho_c$ and one hypothesizes that it does so with a power law: $\rho_a \simeq C(\rho - \rho_c)^\beta$. ρ_c, C, and β are then taken to be the parameters which give the best fit to this relation, using a least-squares fit for the linear relation between $\log \rho_a$ and $\log(\rho - \rho_c)$. With this method we find, from simulations in an $L \times L$ box with $L = 1024$, that (i) for the continuous time models, $\rho_c = 0.3308$ for dynamics defined by rule (1) and $\rho_c = 0.3471$ for rule (2), and (ii) for the discrete time models, $\rho_c = 0.2685$ for rule (1) and $\rho_c = 0.2391$ for rule (2). For all four models the values of β lie in the interval $[0.621, 0.628]$.

3. Phenomenological description

As noted in the introduction, we wish to study the model in the region $\rho \leqslant \rho_c$; from now on we restrict our attention to this region and write $\delta := \rho_c - \rho \geqslant 0$. Let $\mu_t^{(\rho)}$ be the infinite-lattice measure at time t when the initial measure is the Bernoulli (product) measure of density ρ, which we denote $\mu_0^{(\rho)}$, and let

$$\nu_\rho := \lim_{t\to\infty} \mu_t^{(\rho)} \tag{1}$$

be the corresponding final state. We will always assume that ν_ρ is frozen; we know of one model for which this is not true when $\rho = \rho_c$, the 1-d discrete-time symmetric FEP [7], and will describe this in section 6 but not consider it here.

The following picture of the behavior of the variances $V(L)$, under the measure ν_ρ, as $\rho \nearrow \rho_c$, emerges from simulations of the FEP in two dimensions and theoretical considerations in $d = 1$; we discuss it, however, in an arbitrary dimension d. Suppose that $\rho < \rho_c$ and that $\delta \ll 1$. Then:

(P1) There are three regimes in L, which we call regimes of 'small,' 'intermediate,' and 'large' L, although we emphasize that since we are speaking of asymptotic results, our descriptions always assume that L is in fact sufficiently large.

(P2) In the regime of *small* L the variances grow approximately as in the hyperuniform state at ρ_c: $V(L) \simeq C_1 L^{\lambda_1}$ (see section 2).

(P3) At some (approximately defined) scale $L_1 = L_1(\delta)$ the variances enter the regime of *intermediate* L, in which they grow as $V(L) \simeq C_2(\delta) L^{\lambda_2}$ with $\lambda_2 > d > \lambda_1$ and $C_2(\delta) > 0$.

(P4) The growing variances reach size of order L^d at an (approximate) scale $L_2 = L_2(\delta)$; for $L > L_2$, the regime of *large* L, the variances grow so as to coincide, even up to prefactor, with the variances in the initial measure: $V(L) \simeq \rho(1-\rho)L^d$.

(P5) As $\rho \nearrow \rho_c$, $L_1(\delta)$ and $L_2(\delta)$ increase as $L_i \sim \delta^{-\gamma_i}$ for some exponents γ_1, γ_2, with $\gamma_2 > \gamma_1 > 0$.

We illustrate (P1)—(P5) in figure 2, a log-log plot of the variances $V(L)$ in the continuous time, rule (1), 2d FEP for $\delta = 0.1$, 0.01, 0.001, and 0. The data is from a 2048×2048 system. Also shown are the lines $V = C_1 L^{\lambda_1}$ (here $C_1 = 0.104$ and $\lambda_1 = 1.57$), $V = \rho_c(1-\rho_c)L^2$, and, for $\delta = 0.01$, the line $C_2(\delta)L^{\lambda_2}$ (with $C_2(0.01) = 0.0157$, $\lambda_2 = 2.47$) and approximate values of $L_1 = L_1(0.01)$ and $L_2 = L_2(0.01)$. The inset will be discussed below.

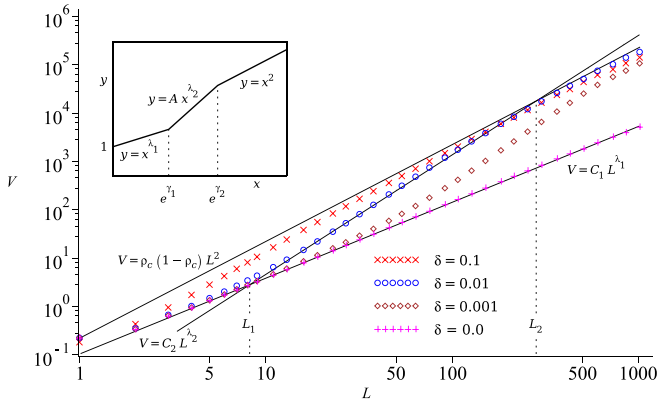

Figure 2. Log-log plot of the variances $V(L)$ in the continuous time rule-(1) 2d FEP for four density values, together with the approximating straight lines giving the power law growth described in (P1)–(P5). The values of L_1, L_2, and C_2 shown correspond to $\delta = 0.01$. The inset shows the conjectured limit of the data under power scaling; if $C_2(\delta) = D\delta^\theta$ as in remark 1 then $A = e^{-\theta}$.

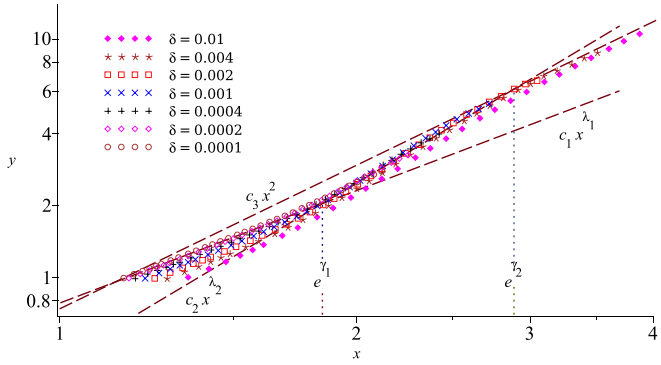

Figure 3. Log-log plot of the variances $V(L)$ in the continuous time rule-(1) 2d FEP after power scaling, for density values $\delta = 0.01$, 0.004, 0.002, 0.001, 0.0004, 0.0002, and 0.0001. Also shown are approximating straight lines giving the power law growth and the approximate values e^{γ_1} and e^{γ_2}, which here correspond to $\gamma_1 \approx 0.61$, $\gamma_2 \approx 1.06$.

Power scaling: We can further justify the conclusions (P1)—(P5) by collapsing the data under an appropriate scaling. In [8] a multiplicative scaling, which in our terms would be $L \to \delta^{\gamma_1} L$, $V \to \delta^{\lambda_1\gamma_1} V$, partially collapses the observed L-V data for the 2d FEP. As remarked there, however, such a scaling cannot give complete collapse, since there are different exponents in the different regimes. Instead we introduce a *power scaling*:

$$(L, V(L)) \to \left(L^{\alpha(\delta)}, V(L)^{\alpha(\delta)}\right), \tag{2}$$

which corresponds to a *linear* rescaling in the log-log plots, carrying straight lines to straight lines of the same slope. The exponent $\alpha(\delta)$ must be chosen so that the scaling limit exists when $\delta \to 0$; we choose $\alpha(\delta) = -(\log\delta)^{-1}$, which leads to limits for the two 'special' points, $(L_1, C_1 L_1^{\lambda_1})$ and (L_2, L_2^d), of figure 2(a):

$$\left(L_1, C_1 L_1^{\lambda_1}\right) \sim \left(\delta^{-\gamma_1}, C_1\delta^{-\gamma_1\lambda_1}\right) \underset{\text{scale}}{\longrightarrow} \left(e^{\gamma_1}, C_1^{\alpha(\delta)} e^{\gamma_1\lambda_1}\right) \underset{\delta\searrow 0}{\longrightarrow} \left(e^{\gamma_1}, e^{\gamma_1\lambda_1}\right), \tag{3}$$

and similarly, under the same scaling and limit, $(L_2, L_2^d) \to (e^{\gamma_2}, e^{\gamma_2 d})$. Thus under this scaling the plot of figure 2 approaches the limit shown in the inset of that figure.

The effect of power scaling for actual data—specifically, that of the continuous time, rule (1) model at seven different densities, from $\delta = 0.01$ to $\delta = 0.0001$—is shown in figure 3. Also shown are approximate values of e^{γ_1} and e^{γ_2} obtained from (3). The constants c_1, c_2, and c_3 used in the figure for the curves $y = c_i x^{\lambda_i}$ are chosen to fit the data shown; in the $\delta \searrow 0$ limit c_1 and c_3 would have value 1, but the logarithmic convergence of $\alpha(\delta)$ to zero with δ is too slow for this limit to be apparent.

Further discussion: The existence of a regime of small L with behavior as described in (P2) can be readily understood, given that hyperuniformity holds for ν_{ρ_c} as described in section 2. For as $\delta \searrow 0$ the state ν_ρ should converge to ν_{ρ_c}, which implies that the distribution under ν_ρ of the number of particles in a box of size L^d, and hence in particular the variance $V(L)$ of that number, should converge to that for ν_{ρ_c}. (Of course for larger and larger L we must require smaller and smaller δ.) Thus for $0 < \delta \ll 1$ we should have that $V(L) \simeq C_1 L^{\lambda_1}$, provided that L is large but not too large.

The fact that the fluctuations are as in the initial measure for sufficiently large L, that is, that as described in (P4), $V(L) \simeq \rho(1-\rho)L^d$ there, is also easily understood. For, since the configurations are becoming frozen as $t \nearrow \infty$, we expect that each particle will, with probability one, move only a finite distance during the evolution. Thus the number of particles in a sufficiently large box is, to high relative accuracy, the same at the end of the evolution as it was at the beginning [6], and the fluctuations in this number should also be the same as for the original Bernoulli measure.

There must thus be a region of transition between the region of small L with slow growth $V(L) \simeq C_1 L^{\lambda_1}$ and the region of large L with normal $\rho(1-\rho)L^d$ growth; the growth in this intermediate region must be faster than $V(L) \simeq \rho(1-\rho)L^d$ to connect the smallish slow-growth variance for small L with the normal growth variance at large L. One possibility is that of (P3), $V(L) \simeq C_2(\delta)L^{\lambda_2}$ with $\lambda_2 > \lambda_1$ and $\lambda_2 > d$, but we see no *a priori* reason for this to hold; one might also have, for example, normal growth $V(L) \simeq CL^d$ with prefactor C larger than $\rho_c(1-\rho_c)$.

Remark 1. Suppose that in fact $V \simeq C_2(\delta)L^{\lambda_2}$ in the intermediate region, as in (P3), and that for some constant D, $C_2(\delta) \simeq D\delta^\theta$ as $\delta \searrow 0$. (This is in fact true for the $d = 1$ case, with $\theta = 1$ and $D = \sqrt{8/\pi}/3$; see section 4). This will then determine the exponents γ_1 and γ_2 of (P5): matching values of $V(L)$ at $L_1(\delta)$ and $L_2(\delta)$ yields $C_1 L_1^{\lambda_1} = D\delta^\theta L_1^{\lambda_2}$ and $\rho_c(1-\rho_c)L_2^d = D\delta^\theta L_2^{\lambda_2}$, from which we obtain that $L_i(\delta) \simeq B_i\delta^{-\gamma_i}$ with

$$\gamma_1 = \theta/(\lambda_2 - \lambda_1), \qquad \gamma_2 = \theta/(\lambda_2 - d), \tag{4}$$

and

$$B_1 = (C_1/D)^{1/(\lambda_2-\lambda_1)}, \qquad B_2 = (\rho_c(1-\rho_c)/D)^{1/(\lambda_2-d)}. \tag{5}$$

However, the status of B_1 and B_2 is somewhat different from that of γ_1 and γ_2, as we discuss in remark 2 in section 4.

4. The FEP in one dimension

We now turn to the FEP in one dimension, that is, on $\mathbb{Z}$, still in continuous time. Note that in this case a particle can jump only if exactly one of its two neighboring sites is occupied, so that at most one jump, either left or right, is possible for each active particle (so there is now no difference between the two dynamical rules (1) and (2) of section 2). For this model we can establish rigorously a slightly modified version of the properties (P1)–(P5), as we now discuss; the proof also determines explicitly the various parameters λ_1, λ_2, C_1, C_2, δ_1, and δ_2 which appear in (P2), (P3), and (P5) and confirms the behavior $V_\rho(L) \simeq \rho(1-\rho)L$ in the region of 'large' L (see (P4)).

In this section we write $V_\rho(L)$ for the variance of the number of particles in an interval of length L under the measure ν_ρ of (1). The key input for our analysis of this quantity is the explicit knowledge [6] of ν_ρ, $\rho \leqslant \rho_c = 1/2$, for this model. As a consequence our results also hold for several other models, for which the measure ν_ρ agrees with that in the 1d FEP, as we discuss in section 6. The measure $\nu_{1/2}$ at the critical density is of special interest:

$$\nu_{1/2} = \frac{1}{2}\left(\delta_{\eta^*} + \delta_{\eta^\dagger}\right), \tag{6}$$

where η^* and $\eta^\dagger$ are the two configurations in which holes and particles strictly alternate. $\nu_{1/2}$ is (trivially) hyperuniform; in particular,

$$V_{1/2}(L) = \begin{cases} \frac{1}{4}, & \text{if } L \text{ is odd,} \\ 0, & \text{if } L \text{ is even.} \end{cases} \tag{7}$$

Plots of $V_\rho(L)$ for four values of ρ are shown in figure 4. (The data plotted in figure 4 were obtained by direct simulation of the known final measure ν_ρ, without actually simulating the time evolution; this method permits the evaluation of $V_\rho(L)$ for large values of L.) It is clear that the behavior of $V_\rho(L)$, in contrast to that of the variances in the models discussed in section 3, depends, for small L, on whether L is even or odd; this may be thought of as the legacy, at small values of δ, of the $\delta = 0$ behavior of (7). Moreover, from the figure we can observe that:

- For odd L the variances appear to behave as described in (P1)–(P5), with $C_1 = 1/4$, $\lambda_1 = 0$ and $\lambda_2 = 3/2$.
- For even L the 'small' growth region described by (P2) is absent: for small and moderate values of L the variances grow as $C_2(\delta)L^{3/2}$.
- The values of δ used in the figure differ by factors of 10, as do the (approximate) straight lines $C_2(\delta)L^{3/2}$ giving $V(L)$ in the intermediate (and low, for L even) density region. This suggests that $C_2(\delta)$ vanishes linearly in δ as $\delta \searrow 0$: $C_2(\delta) = D\delta$ for some constant D. From (4) we then have $\gamma_1 = 2/3$ and $\gamma_2 = 2$.

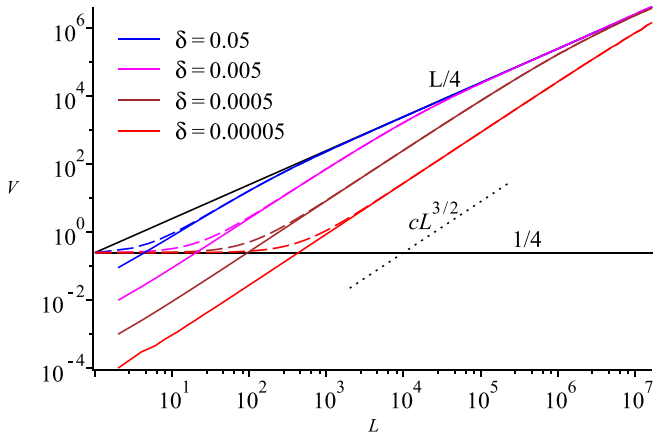

Figure 4. Variances in the 1d FEP for four values of the density. The solid curves correspond to even values of L, the dashed ones to odd values. The black lines are for comparison purposes: $V = 1$, $V = L/4$, and $V = cL^{3/2}$ (dotted).

The following result, whose proof will appear in a subsequent publication, gives a formal description of this behavior as well as the value of the constant D:

Theorem 1. *Let N_L be the number of particles on the sites $1, 2, \ldots, L$ for the FEP with density $\rho = 1/2 - \delta$, $0 < \delta < 1/2$. Then:*

(a) For L odd,

$$\mathrm{Var}_{\nu_\rho}(N_L) \simeq \begin{cases} \frac{1}{4}, & \text{for } L \ll \delta^{-2/3}, \\ \frac{2}{3}\sqrt{\frac{2}{\pi}}\delta L^{3/2}, & \text{for } \delta^{-2/3} \ll L \ll \delta^{-2}, \\ \frac{1}{4}L, & \text{for } L \gg \delta^{-2}. \end{cases} \tag{8}$$

(b) For L even,

$$\mathrm{Var}_{\nu_\rho}(N_L) \simeq \begin{cases} \frac{2}{3}\sqrt{\frac{2}{\pi}}\delta L^{3/2}, & \text{for } 1 \ll L \ll \delta^{-2}, \\ \frac{1}{4}L, & \text{for } L \gg \delta^{-2}. \end{cases} \tag{9}$$

Here we are using a slight extension of our earlier notation: if $A(\delta, L)$ and $B(\delta, L)$ are real valued functions whose asymptotic behavior in L we wish to compare, and $K(\delta)$ is a positive function, then we write $A(\delta, L) \simeq B(\delta, L)$ for $L \ll K(\delta)$ (respectively for $L \gg K(\delta)$) if for any $\epsilon > 0$ there exists a $\delta_0 > 0$ and a number $t > 0$ such that $1 - \epsilon < A(\delta, L)/B(\delta, L) < 1 + \epsilon$ when $\delta < \delta_0$ and $L < tK(\delta)$ (respectively $L > tK(\delta)$).

Remark 2. As mentioned in remark 1, the B_i of (5) have a somewhat different status from the γ_i of (4), as we now discuss in the context of the 1d model. The latter are unambiguously determined by theorem 1, since (8) and (9) would be false for any $\gamma_1 \neq 2/3$ and/or $\gamma_2 \neq 2$ (indeed, even for the 2d

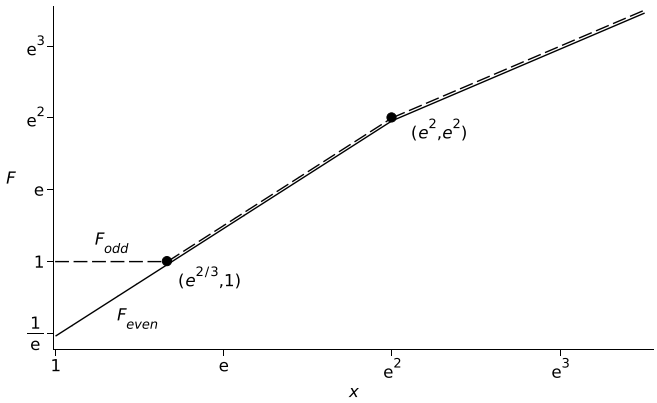

Figure 5. Log-log plot of the limiting functions F_{odd} and F_{even} under power scaling. Compare with the inset in figure 2.

model the values of these exponents are fairly clear directly from the data (see figure 3)). But this is not true for B_1 and B_2, since (8) and (9) are compatible with any choices of constant coefficients in front of the powers of δ in the L-ranges of these equations. No dramatic change in the behavior of the variance occurs exactly at the $L_i = B_i\delta^{-\gamma_i}$, and we do not know the size of the transition regions between 'small' and 'intermediate' and between 'intermediate' and 'large'. The theorem itself is compatible with these regions being very large indeed. Nevertheless, we emphasize that the B_i are sharply defined, as described in remark 1, as giving the locations of the intersections of the asymptotics for the three regions.

It is an immediate consequence of theorem 1 that the plots of $V_\rho(L)$ against L (figure 4) collapse under the power scaling (2). Specifically, if as $\delta \to 0$, $L \to \infty$ through odd (respectively even) values in such a way that $L^\alpha \to x$ (with $\alpha = \alpha(\delta) = -1/\log\delta$), then $V_\rho(L)^\alpha \to F_{\text{odd}}(x)$ (respectively $V_\rho(L)^\alpha \to F_{\text{even}}(x)$), with

$$F_{\text{even}}(x) = \begin{cases} e^{-1}x^{3/2}, & \text{for } 1 \leqslant x \leqslant e^2, \\ x, & \text{for } e^2 < x; \end{cases} \tag{10}$$

$$F_{\text{odd}}(x) = \begin{cases} 1, & \text{for } 1 \leqslant x \leqslant e^{2/3}, \\ F_{\text{even}}(x), & \text{for } e^{2/3} < x. \end{cases} \tag{11}$$

The limiting functions F_{even} and F_{odd} are plotted in figure 5.

5. Sketch of the proof

In this section we wish to give some hints as to how theorem 1 can be established, with particular emphasis on a heuristic discussion of the $V_\rho(L) \simeq D\delta L^{3/2}$ behavior in the intermediate-L (and, for L even, low-L) region. For (setting aside any difficulties in giving formal proofs) the behavior $V_\rho(L) \simeq 1/4$ for L odd and 'small' (that is, $L \ll \delta^{-2/3}$) is readily understood in terms of the $\delta = 0$ behavior (7) and the discussion in section 3. The behavior for 'large' L, $L \gg \delta^{-2}$, is also discussed in section 3; on a more formal level, it is proved in [6] that

$$\lim_{L\to\infty} \frac{V_\rho(L)}{L} = \rho(1-\rho), \tag{12}$$

which is almost the result of theorem 1, lacking only the uniformity as $\delta \searrow 0$ with which the limit is achieved.

In the remainder of this section we take L to be a variable satisfying $1 \ll L \ll \delta^{-2}$. We will freely drop lower-order terms, approximate sums by integrals, etc; these manipulations can all be justified.

The key ingredient for understanding the $L^{3/2}$ behavior is the renewal structure of the stationary state ν_ρ, $\rho < 1/2$. In this state adjacent 1's have probability zero; thus the state is supported on configurations of the form

$$\cdots 1\,0\,1\,0\,1\,0\,1\,0\,\hat{0}\,1\,0\,1\,0\cdots 1\,0\,\hat{0}\,1\,0\,1\,0\,1\,0\cdots 1\,0\,\hat{0}\cdots \tag{13}$$

$$= \cdots 0\ (1\,0\,)^{X_{-1}}\ 0\ (1\,0)^{X_0}\ 0\ (1\,0)^{X_1}\ 0\ (1\,0)^{X_2}\,0\cdots. \tag{14}$$

For ν_ρ the 00's in (13)—or more specifically the second 0 of such pair, marked as $\hat{0}$ in (13) and corresponding to a 0 outside the parentheses in (14)—are the *renewal events* of a *renewal process* [6]. This means that, if we condition on the occurrence of a such an event at the origin, so that the X_i may be well defined—for example by noting that renewal events are separated by distances $2X_i + 1$, and letting $2X_1 + 1$ be distance from the origin to the first renewal event on the right—then the X_i are independent random variables that are identically distributed.

The independence of the X_i is easily understood: because adjacent empty sites cannot be created during the evolution, the double zeros in (13) must have been present for all t, $0 \leqslant t < \infty$, so that the portions of the system to the left and right of each, independent under the initial Bernoulli measure, evolve independently. Note that since under ν_ρ the probability that a site is occupied is ρ and the probability of occupied adjacent sites is zero, the density of the renewal events is $1 - 2\rho = 2\delta$.

The distribution of the X_i is that of a random variable X with

$$P(X=n) = C_n\rho^n(1-\rho)^{n+1} = \frac{1+2\delta}{2\cdot 4^n}C_n\left(1-4\delta^2\right)^n, \quad n = 0,1,2,\ldots \tag{15}$$

where C_n is the nth Catalan number,

$$C_n = \frac{1}{n+1}\binom{2n}{n} \simeq \frac{4^n}{n^{3/2}\sqrt{\pi}}. \tag{16}$$

In (16) we have used Stirling's formula. Thus for $n \gg 1$ and $\delta \ll 1$,

$$P(X=n) \simeq \frac{1+2\delta}{2n^{3/2}\sqrt{\pi}}\left(1-4\delta^2\right)^n \simeq \frac{1}{2n^{3/2}\sqrt{\pi}}e^{-4\delta^2 n}. \tag{17}$$

We see that if δ is zero then X_i has power-law distribution with a long tail (in particular, with infinite expectation), but that for positive δ the distribution is cut off at order $n \approx \delta^{-2}$.

Now let N_L and R_L denote respectively the number of particles and the number of renewal events in the interval $\{1,\dots,L\}$. It is easy to see that

$$N_L = \frac{1}{2}\left(L - R_L - \sigma\right), \tag{18}$$

where σ may take value 0, 1, or -1, and thus

$$\mathrm{Var}\left(N_L\right)\ (= V_\rho\left(L\right)) \simeq \frac{1}{4}\mathrm{Var}\left(R_L\right), \tag{19}$$

up to a correction arising from σ. We will show (heuristically) below, and prove rigorously elsewhere, that

$$\mathrm{Var}\left(R_L\right) \simeq \frac{8}{3}\sqrt{\frac{2}{\pi}}\delta L^{3/2} \quad \left(L \ll \delta^{-2}\right); \tag{20}$$

we will also prove elsewhere that the correction to (19) arising from σ is negligible for L even and is $1/4$ (up to order δ) for L odd. This gives a heuristic justification of the $L \ll \delta^{-2}$ cases of theorem 1.

We now consider (20). Let S_L be the number of renewal events in $\{1,\dots,L\}$, *conditioned on the occurrence of a renewal event at the origin*. We can express the moments of R_L in terms of those of S_L by conditioning on the value Y of the position of the first renewal event to the right of the origin ($Y \geqslant 1$):

$$E\left(R_L^k\right) = \sum_{y=1}^{L} P\left(Y=y\right) E\left(\left(1+S_{L-y}\right)^k\right), \qquad k=1,2,\dots, \tag{21}$$

where E denotes expectation (and we have set $S_0 = 0$). Note that the equality in (21) does not hold for $k=0$, because the terms with $y > L$ are omitted from the sum, but that this omission does not matter for $k \geqslant 1$ because $R_L = 0$ if $Y > L$.

To obtain $P(Y=y)$ we note that, given that there is a renewal event at $-m$, $m \geqslant 0$, which happens with probability 2δ, the probability that this is the first renewal event at or to the left of the origin, and that $Y=y$, is $P(X=(m+y-1)/2)$ (and in particular is 0 unless m and y have different parities). Thus using (17) we have, for $\delta \ll 1$,

$$\begin{aligned} P\left(Y=y\right) &= 2\delta \sum_{m\geqslant 0,\ m+y \text{ odd}} P\left(X = \frac{m+y-1}{2}\right) \\ &\simeq \frac{\delta}{\sqrt{\pi}} \sum_{n \geqslant y/2} \frac{1}{n^{3/2}} \simeq \frac{\delta}{\sqrt{\pi}} \int_{y/2}^{\infty} \frac{\mathrm{d}u}{u^{3/2}} = 2\delta\sqrt{\frac{2}{\pi y}}. \end{aligned} \tag{22}$$

The moments of S_L, the other ingredient in (21), may be obtained from section 3(ii) of [5], once one makes the approximation that the distance between renewal events is distributed as $2X$ (rather than $2X+1$), where now X is the random variable having distribution (15) with $\delta = 0$. For it is shown there that then $S_L \simeq \sqrt{L}|Z|$, with Z a standard normal random variable, so that

$$E\left(S_L^2\right) \simeq L. \tag{23}$$

Now substituting (22) and (23) into (21) we have, using $1 + S_{L-y} \simeq S_{L-y}$,

$$\begin{aligned} E\left(R_L^2\right) &\simeq \frac{2\sqrt{2}\delta}{\sqrt{\pi}} \int_0^L \frac{L-y}{\sqrt{y}}\,\mathrm{d}y = \frac{2\sqrt{2}\delta L^{3/2}}{\sqrt{\pi}} \int_0^1 \frac{1-u}{\sqrt{u}}\,\mathrm{d}u \\ &= \frac{8}{3}\sqrt{\frac{2}{\pi}}\delta L^{3/2}. \end{aligned} \tag{24}$$

Since $L \ll \delta^{-2}$, $E(R_L)^2 = (2\delta L)^2 \ll E(R_L^2)$, and so $\mathrm{Var}(R_L) \simeq E(R_L^2)$, yielding (20).

It is instructive to note that the probability of at least one renewal event in $\{1,\dots,L\}$ is

$$\begin{aligned} P\left(R_L > 0\right) &= \sum_{y=1}^{L} P\left(Y=y\right) \simeq 2\delta \int_1^L \sqrt{\frac{2}{\pi y}}\,\mathrm{d}y \\ &\simeq 4\delta\sqrt{\frac{2}{\pi}}\sqrt{L} \ll 1, \end{aligned} \tag{25}$$

where we have used $L \ll \delta^{-2}$; thus an interval of L sites typically contains no renewal events.

An unexpected connection: Within the renewal process framework just described there is a strong connection between the exponent λ_2 in the region of 'intermediate' L and the coefficient C_3 in the growth relation $V(L) \simeq C_3 L$ for 'large' L. Specifically, the fact that C_3 is bounded away from 0 and ∞ as $\delta \searrow 0$ corresponds, in a sense that we now make precise, to the value $\lambda_2 = 3/2$ of the 1d FEP.

Consider then a process of renewal events as described above, but based on a renewal random variable X with distribution

$$P\left(X=n\right) = \frac{A\left(\Lambda\right)}{n^\gamma} e^{-n/\Lambda}, \quad n = 1,2,3,\dots, \tag{26}$$

with $1 < \gamma < 2$ and $A(\Lambda)$ a normalization constant (compare with (17), which corresponds to $\gamma = 3/2$, $\Lambda = (2\delta)^{-2}$). For simplicity we assume that X itself, rather than $2X+1$, gives the distance between renewal events; since $E(X) \sim \Lambda^{2-\gamma}$ these events have density $\delta \sim \Lambda^{\gamma-2}$. We are interested in the behavior of this process as $\Lambda \nearrow \infty$ (note that $A(\Lambda)$ is finite and nonzero in this limit).

For $L \ll \Lambda$, which here corresponds to the 'intermediate' region, we may repeat the calculations above. Now (22) becomes $P(Y=y) \sim \delta / y^{\gamma-1}$, and since $E(S_L^2) \sim L^{2(\gamma-1)}$ from [5], following (24) we find that $E(R_L^2)$ is of order

$$\delta \int_0^L \frac{(L-y)^{2(\gamma-1)}}{y^{\gamma-1}}\,\mathrm{d}y = \delta L^\gamma \int_0^1 \frac{(1-u)^{2(\gamma-1)}}{u^{\gamma-1}}\,\mathrm{d}u, \tag{27}$$

i.e. of order δL^γ. Since $E(R_L)^2 = (\delta L)^2 \ll \delta L^\gamma$, $\mathrm{Var}(R_L)$ is of this same order; thus $\lambda_2 = \gamma$.

The asymptotic value of $\mathrm{Var}(S_L)$ is obtained in [4] (see problems (19)–(23) of chapter XIII) and the same methods may be used to determine $\mathrm{Var}(R_L)$:

$$\mathrm{Var}\left(R_L\right) \simeq \frac{\mathrm{Var}\left(X\right)}{E\left(X\right)^3} L. \tag{28}$$

(In fact, (28) also holds with $\mathrm{Var}(R_L)$ replaced by $\mathrm{Var}(S_L)$). We observed above that $E(X) \sim \Lambda^{2-\gamma}$, and a similar calculation shows that $E(X^2) \sim \Lambda^{3-\gamma}$ and so also $\mathrm{Var}(X) \sim \Lambda^{3-\gamma}$, so that from (28), $\mathrm{Var}(R_L) \sim \Lambda^{2\gamma-3}L$. Thus the coefficient of L in the region of 'large' L is of order unity as $\Lambda \nearrow \infty$ precisely when the 'intermediate' region exponent $\lambda_2 = \gamma$ has value $3/2$.

6. Related models and open problems

As indicated in section 4, the results that we describe there and in section 5 apply to several other one-dimensional models. The continuous time model that we treat in sections 3–5, in which particles jump to all directions at equal rates, may be generalized in one dimension to the *partially asymmetric* model, in which left and right jumps occur at different rates. These models again have an absorbing phase transition at $\rho_c = 1/2$, and it is shown in [1] that the limiting measure ν_ρ for $\rho < 1/2$ (and indeed for all ρ) is independent of the degree of asymmetry, so that for $\rho < 1/2$ it is the measure analyzed in section 5. The latter result is also true in discrete time for the *totally* asymmetric FEP [6], in which particles jump only to the right and then, of course, only if their left-hand neighboring site is occupied (although here the $\rho > 1/2$ measures do not coincide with those of the continuous time model). Thus theorem 1 holds for all these models.

Given the above, we can understand the structure of the measure ν_ρ, $\rho < 1/2$, described in section 5, by viewing it as the limiting measure for the totally asymmetric model. To do so we associate with each initial configuration of that model a random walk on the integers, in which the walker takes a step to the right (respectively left) at time i if and only if site i is empty (respectively occupied). Since $\rho < 1/2$ the walk has a drift to the right. It is then easy to convince oneself that the final configuration is completely determined by the initial one, and that the renewal events in (13) occur at sites i such that the random walk reaches a new maximum at time i. The intervals between two such maxima, which have the form $2X_i + 1$ in (14), are certainly independent, and their distribution (15) is determined by the well-known fact that the Catalan number C_n counts the number of walks (*Dyck paths of length* $2n$) between two such maxima which are separated by a distance $2n + 1$.

The situation is different for the *symmetric* discrete-time model in one dimension [7] (partially asymmetric discrete-time models have not been studied, to our knowledge). In contrast to the models discussed in the previous paragraph, adjacent empty sites can be created during the evolution, and the measure ν_ρ of section 5 is no longer the limiting measure. In particular, at $\rho = 1/2$, where the measure (6) is the unique translation invariant stationary (TIS) measure for the models of the previous paragraph, now there are two uncountable families of extremal TIS measures, each in correspondence with the set of all TI measures on $\{0,1\}^{\mathbb{Z}}$; these describe situations in which patterns formed by occupied and unoccupied sites move to the left or right, respectively, with velocity 2. It is shown in [7] that $\lim_{t\to\infty} \mu_t^{(\rho)}$ exists for $\rho < 1/2$, but little is known about the nature of the limiting measure. For $\rho = 1/2$ the existence of the limit is not proven; if it exists it must of course be a convex combination of the extremal TIS measures mentioned above, and simulations suggest a highly nontrivial combination.

Hexner and Levine [8] study several models, other than the FEP, which exhibit a phase transition to an absorbing state: the Manna model in one dimension and the 'random organization' model in both one and two dimensions. In all cases they find that the state at the critical value of the density is hyperuniform. Their plots showing the dependence of the fluctuations on L and on the density are generally similar to our figure 2, so we suspect that the phenomenology that we describe in section 3 will apply there, also, but we have not investigated the question.

The complete absence of theoretical results for the FEP models in dimensions two and higher presents a challenge to mathematical physicists. For example, one would very much like to have a proof of the existence of active states at some density below $1/2$ and/or, conversely, a proof that the system must freeze when started from a Bernoulli initial distribution of sufficiently low density ρ (say, $\rho < 10^{-23}$). On a more refined level one would like to establish the existence of a critical density $\rho_c < 1/2$ such that final states are frozen for $\rho < \rho_c$ and active for $\rho > \rho_c$, and then prove that, as suggested by simulations, the final state at ρ_c is frozen and hyperuniform.

Data availability statement

The data cannot be made publicly available upon publication because they are not available in a format that is sufficiently accessible or reusable by other researchers. The data that support the findings of this study are available upon reasonable request from the authors.

ORCID iD

E R Speer https://orcid.org/0000-0003-3614-5597

References

[1] Ayyer A, Goldstein S, Lebowitz J L and Speer E R 2023 Stationary states of the one-dimensional facilitated asymmetric exclusion process *Ann. Inst. Henri Poincaré* B **59** 728–42
[2] Blondel O, Erignoux C, Sasada M and Simon M 2020 Hydrodynamic limit for a facilitated exclusion process *Ann. Inst. Henri Poincaré Probab. Stat.* **56** 667714
[3] Blondel O, Erignoux C and Simon M 2021 Stefan problem for a non-ergodic facilitated exclusion process *Probab. Math. Phys.* **2** 127–78
[4] Feller W 1968 *An Introduction to Probability Theory and Its Applications, Volume I* 3rd edn (Wiley)
[5] Godrèche C and Luck J M 2001 Statistics of occupation time of renewal processes *J. Stat. Phys.* **104** 489–524
[6] Goldstein S, Lebowitz J L and Speer E R 2021 The discrete-time facilitated totally asymmetric simple exclusion process *Pure Appl. Funct. Anal.* **6** 177–203 (available at: http://yokohamapublishers.jp/online2/oppafa/vol6/p177.html)

[7] Goldstein S, Lebowitz J L and Speer E R 2022 Stationary states of the one-dimensional discrete-time facilitated symmetric exclusion process *J. Math. Phys.* **63** 083301
[8] Hexner D and Levine D 2015 Hyperuniformity of critical absorbing states *Phys. Rev. Lett.* **114** 110602
[9] Lee T D and Yang C N 1952 Statistical theory of equations of state and phase relations II: lattice gas and Ising model *Phys. Rev.* **87** 410–9
[10] Liggett T M 1985 *Interacting Particle Systems* (Springer)
[11] Lübeck S 2001 Scaling behavior of the absorbing phase transition in a conserved lattice gas around the upper critical dimension *Phys. Rev.* E **64** 016123
[12] Oliveira M J 2005 Conserved lattice gas model with infinitely many absorbing states in one dimension *Phys. Rev.* E **71** 016112
[13] Presutti E and Spohn H 1983 Hydrodynamics of the voter model *Ann. Probab.* **11** 867–75
[14] Rossi M, Pastor-Satorras R and Vespignani A 2000 Universality class of absorbing phase transitions with a conserved field *Phys. Rev. Lett.* **85** 1803
[15] Torquato S 2018 Hyperuniform states of matter *Phys. Rep.* **745** 1–95